

Expired *GlucoredForte* Drug: Eco-Friendly Corrosion Inhibitor for Mild Steel

ABSTRACT

Expensive casualties can occur if the basic corrosion control technology does not properly check. Repurposing expired *GlucoredForte* drugs as corrosion inhibitor reduces waste and promotes environmental sustainability. The present work investigated the corrosion inhibition of mild steel using an expired *GlucoredForte* drug in 2 M HCl solution. The inhibitive properties of mild steel in 2 M HCl solution were evaluated at various temperature range of 30°C – 50°C using weight loss measurements. The expired *GlucoredForte* drug showed efficiency of 85.7% at concentration of 300ppm. The spontaneous adsorption of the *GlucoredForte* drug on a mild steel surface is indicated by the negative values of Gibb's free energy (ΔG°_{ads}) which ranged from -14.52 kJ/mol to -22.57 kJ/mol, and the mechanism of adsorption is physisorption. The endothermic process of the adsorption of the *GlucoredForte* drugs on the mild steel surface is shown by the positive values of ΔH° . The negative values for entropy entail that the adsorption behaviour is accompanied by a decrease in entropy. The results showed that inhibition efficiency increased with increase in concentration of inhibitors and decreased with increase in temperature. The presence of heteroatoms such as Nitrogen and Oxygen, as well as the presence of π -bonds in the aromatic rings strengthened the observable effect of Glibenclamide molecule and facilitated surface interaction.

Keywords: mild steel, enthalpy, entropy, drug

1. INTRODUCTION

"Costly crisis can result in negligence of the crucial corrosion guard technology. This is why corrosion protection techniques are to be considered at the stage of design to avoid casualties. Protection of metals is of technical, economic, environmental, and aesthetical importance. One of the best choice of protecting metals and alloys against corrosion are the use of inhibitors" [1-3, 31].

"One of the hazardous materials in the surroundings is the expired drugs which cause the death of over 2000 children every year" [55]. "The expired drugs were wasted in the holes in a desert in some countries which leads to the pollution of the underground water" [4 -10, 12, 50,51,52,53, 55]. This problem draws the attentions of Reda Abdel Hameed [55] to search for the new applications of the expired drugs, and was used first time as corrosion inhibitors for the metals and alloys by Abdelhameed 2009 and 2011, [11-16,17]. "The expired ranitidine drugs was applied as potential nontoxic eco-friendly inhibitor for the corrosion of aluminum in hydrochloric acid solution, his work drawn the attention of the several other scientists and researchers to study many of the expired drugs materials as corrosion inhibitors"[16-21]. "In recent years, many scientists in the field of corrosion inhibition are looking at the eco-friendly and potential nontoxic corrosion inhibitors known as green corrosion inhibitors. One of the most recent efforts is the use of expired drugs to solve not only the problem of soiled waste accumulations but also to produce a potential nontoxic corrosion inhibitor. The application of expired drugs in the protection of metals follows the green chemistry concepts. It was also noted that, the process of using expired drugs as corrosion inhibitors does not involve any waste for as it was taken from the drug market directly to the laboratory, where it was used in their pharmacological form in very few concentrations which is safe for humans and the environment" [2, 55 - 62].

This work is aimed at recycling the expired Glucored Forte drugs as eco-friendly corrosion inhibitor for the mild steel used in manufacturing of petroleum pipe lines. "In addition, the deformation capacity of expired *Glucored Forte* drug to stick to the mild steel surface shall be explored through the DFT method" [54]. The organic molecule structure (Glibenclamide) present in expired *Glucored Forte* drug is as shown in Figure 1.

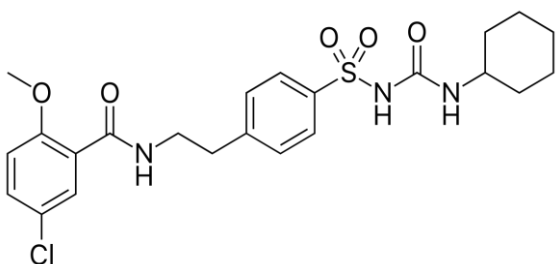


Figure 1: Structure of glibenclamide molecule

2. METHODOLOGY

2.1 Material preparation

The mild steel coupons of dimensions 5cm x 4cm were mechanically press-cut. These coupons were buffed with SiC abrasive paper, degreased in ethanol, dried in acetone, weighed and stored in a moisture free desiccator. [20-22].

2.2 Preparation of Solutions

2 M HCl solution was prepared with distilled water and a calculated amount of the raw acid solution. The expired Glucored Forte drug was prepared in concentrations ranging from 100ppm to 300ppm and a solution without the presence of expired Glucored Forte drugs was taken and kept for reference as the Blank solution. "Tests were conducted under total immersion conditions in 100ml of the test solutions maintained at 30-50°C. The pre-cleaned and weighed coupons were immersed totally in beakers containing the test solutions" [23].

2.3 Determinations of Corrosion Rates

Weight loss variations were monitored at intervals of 2 hours, for a total of 8 hours. After a predetermined time, the mild steel specimens immersed were removed from the test solutions, scrubbed with iron sponge and washed with acetone to remove traces of moisture. The mild steel specimens were then re-weighed. From the change in the weights of the specimens, the corrosion rates were calculated by the formula used in Essien *et al.* [28]:

2.4 Molecular modeling

The computation of semi-empirical parameters for the molecule was done using the PM7 Hamiltonian in the STO-6G software. The molecular mechanics, *Ab initio*, and DFT level were used for the full optimization. The Hyperchem release 8.2 package was used to carry out the single point DFT calculations. "DFT settings (MP2 inclusive) in the package were, Basic set: 321-G, iteration = 50, spin pairing = unrestricted Hartree Fock, convergence limit = 1E-0.05 and Spin multiplicity = 1 (for zero charge and 2 for +1 and -1 charges)" [54].

3. RESULTS AND DISCUSSION

3.1 Gravimetric studies

The gravimetric experiment was carried out and the expired Glucored Forte drug was used as the inhibitor [54]. It was observed that the weight loss measurements increase with an increase in time but decrease with an increase in concentrations of the expired *Glucored Forte* drug (Table 1). Many researchers also reported a similar observation [54]. The weight loss measurements with time at 30° C is shown in Figure 2, and related trends were observed at 40°C and 50°C.

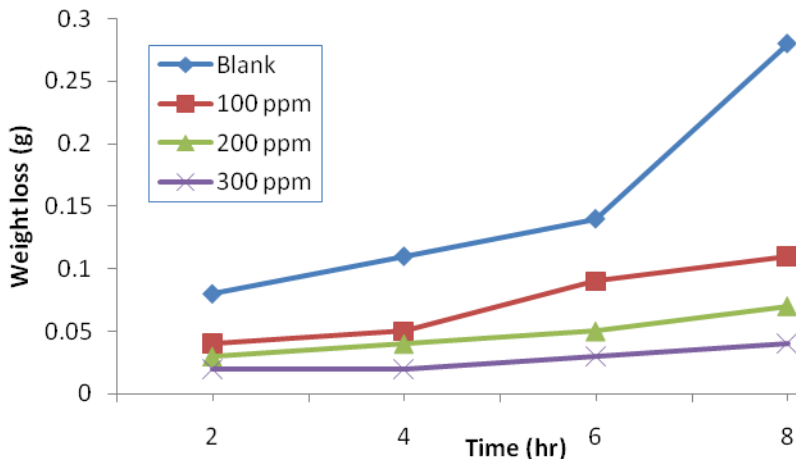


Figure 2: Weight loss versus Time in the absence and presence of different concentrations of expired *Glucored Forte* at 30°C.

Table 1: Calculated values of inhibition efficiency (%), surface coverage (θ) and corrosion rate (CR) of mild steel corrosion in different concentration of GLU

Inhibitor	Conc. (ppm)	303 K			313 K			323 K		
		CR (mm/yr)	θ	I (%)	CR (mm/yr)	θ	I (%)	CR (mm/yr)	θ	I (%)
		$\times 10^{-3}$			$\times 10^{-3}$			$\times 10^{-3}$		
Blank	1.750	-	-	1.380	-	-	2.000	-	-	
GLU	100	0.686	0.608	60.8	0.563	0.592	59.2	0.930	0.532	53.2
	200	0.438	0.750	75.0	0.500	0.678	67.8	0.810	0.594	59.4
	300	0.250	0.857	85.7	0.438	0.683	68.3	0.680	0.656	65.6

The Glucored Forte drug displays corrosion-inhibiting effects at all concentrations reaching a maximum inhibition efficiency of 85.7 % at the concentration of 300 ppm and more efficient at 303 K (Table 1). A similar result was also reported by Paul et al. [26], Essien et al. [28] and Dohare et al. [29], and it indicates partial desorption of the molecules from the Mild Steel surface [54].

3.2 Temperature effect

The gravimetric measurements were carried out in order to study the temperature dependence [29]. The table 1 shows the inhibition efficiencies as a function of concentrations. From table 1, it is shown that the inhibition efficiency increased with increase in the concentration of the inhibitor [30]. This is also observed in most literature [16,29,31–34]. The surface

coverage of the substrate by Expired *Glucoredforte* Drugs attended an optimum level within 8 h. This was noticed with the high efficiency of 85.7 % after 8 h. The results indicate that the highest concentration of the Expired *Glucoredforte* Drugs at 303 K gives maximum inhibition efficiency. It was reported by The Mechanism of physisorption was observed as the results showed that inhibition efficiency decreases with increase in temperature. A similar result was observed by Khaled et al. [19]. It could be examined from the results that inhibitor concentrations increase as the corrosion rates decreases, thus leading to an increase in the inhibition efficiency. The adhesion of Expired *Glucoredforte* Drug molecules on mild steel surfaces were studied using adsorption isotherms [20,21,35] and Essien et al [28]. The interaction of metal surfaces and inhibitor as reported by Umoren [11] are well understood by Adsorption isotherms. The degree of surface coverage values (θ) at different inhibitor concentrations in 2 M HCl solutions were evaluated from gravimetric measurements at 303 K – 323 K and tested graphically for fitting to a suitable adsorption isotherm [20- 23,25,27,31, 54].

The Temkin isotherm model was best fitted with correlation coefficients (R^2) ranging from $0.9952 \geq R^2 \geq 1.0000$. A similar observation was made by Obot and Obi-Egbedi [23]. The low values of K_{ads} indicates weak interaction between the Expired *Glucoredforte* Drug molecules and the mild steel surface which entails electrostatic interaction (Physisorption) [24,36]. The spontaneous process was due to the negative values of ΔG°_{ads} [25,30,31, 54].

Table 2: Adsorption parameters from Temkin isotherm for Mild steel coupons in 2 M HCl containing different concentration of expired GlucoredForte drug at 30-50°C.

Temp. (K)	ADSORPTION PARAMETERS				
	Slope	Intercept	K_{ads}	$-\Delta G(KJ/mol)$	R^2
303	0.125	0.49	50.40	19992.85	0.9952
313	0.045	0.55	202804.96	42251.65	0.9959
323	0.060	0.47	2514.93	31812.54	1.0000

In Table 3, the activation energy values increase in the presence of expired Glucored Forte drug. The adsorption of the expired Glucored Forte drug took place on the higher energy sites. The blocking of the active sites was related to an increase in the activation energy of mild steel corrosion in the inhibited state [37]. The higher value of E_a in the presence of inhibitor compared to that in its absence and the decrease in the inhibition efficiency (%) with rising in temperature is deduced as an indication of physisorption [54, 60 - 62].

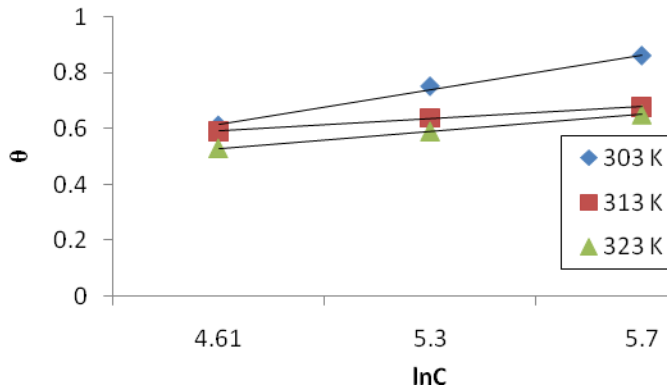


Figure 3: Temkin adsorption isotherm plot as θ versus $\ln C$ for Mild steel coupons in 2 M HCl solution containing different concentration of expired Glucored Forte drug.

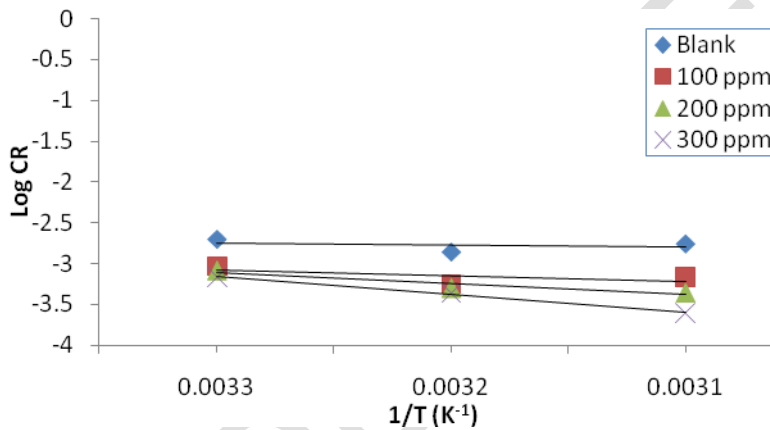


Figure 4: Arrhenius plot as $\log CR$ versus $1/T$ for mild steel coupons in 2 M HCl containing different concentration of expired *Glucored Forte* drug.

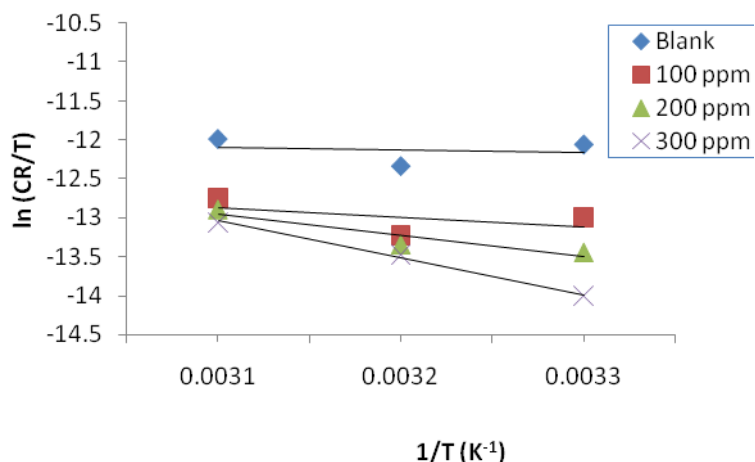


Figure 5: Transition State plot as log (CR/T) versus 1/T for mild steel coupons in 2 M HCl containing different concentration of expired Glucored Forte drug.

The figure 5 showed the transition state plot [6,31]. In table 3, the computed values of the activation parameters for the dissolution of mild steel at various temperatures are shown. "The positive values of ΔH° and negative values of the ΔS° in table 3 reflects the endothermic behavior of the adsorption of the expired Glucored Forte drug on the mild steel surface [22,25,28]. The interaction of the organic compound in the aqueous phase [org (sol)] and water molecules at the electrode surface [$H_2O(ads)$] is considered as a quasi-substitution process" [30]. As such, the adsorption of expired *Glucored Forte* drug is accompanied by desorption of water molecules from the surface of metal steel [54, 57-59].

Table 3: Activation parameters for Mild steel in 2 M HCl containing different concentrations of expired Glucored Forte drug at 30-50°C.

expired Glucored Forte drug Conc. (ppm)	ACTIVATIONPARAMETERS			
	ΔH (KJ/mol)	ΔS (J/mol K ⁻¹)	Ea (KJ/mol)	A x 10 ⁻³ (J/mol K ⁻¹)
Blank	0.5641	85.05	0.2893	0.0015
100	1.3090	79.35	1.0235	0.0005
200	2.6141	79.95	2.3080	0.0003
300	4.2732	80.83	3.9392	0.0002

The algebraic sum of the adsorption of the expired Glucored Forte drug and desorption of water molecules are the obtained thermodynamic parameters [37]. Hence, the increase in entropy is due to the increase in solvent entropy [38, 39, 56].

3.3 Global molecular reactivity

In Table 4, the quantum chemical parameters were computed using the STO-6G software [28,40]. The figures 7 and 8 showed the HOMO and LUMO molecular orbitals of the Glibenclamide molecule respectively. The positive and negative sites of adsorption are represented by the blue and maroon orbitals respectively. The difference in energy of the highest occupied molecular orbital (EHOMO) and that of the lowest unoccupied molecular orbital (ELUMO) defined the reactivity of a chemical species.

Table 4: Molecular properties of Glibenclamide calculated using DFT at the RHF/STO-6G* basis in aqueous phase

	E_{HOMO} (eV)	E_{LUMO} (eV)	ΔE (eV)	M (debye)	IE (eV)	AE (eV)	χ (eV)	η (eV)	S (eV) ⁻¹	ω (eV)	ΔE_{b-d} (eV)
GLI	-0.1394	-0.0467	-0.0927	4716.06	0.1394	0.0467	0.0931	0.0464	21.58	-0.0233	-0.0116

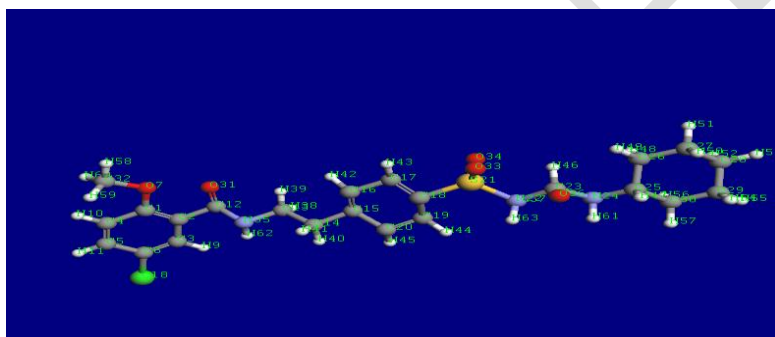


Figure 6: The optimized geometries of the Glibenclamide molecule.

The theoretical aspect of the Glibenclamide molecule was examined with DFT method at the RHF/STO-6G* level. The electronic parameters of the molecule were correlated with inhibition efficiencies. Quantum chemical parameters like EHOMO, ELUMO, dipole moment, energy gap, ionization energy, electron affinity, etc. were obtained in this study. It could be seen in figure 7, that the HOMO is distributed around the central aromatic ring of benzene and Sulphur atom of the molecule, whereas the LUMO shown in figure 8 is distributed around the central aromatic ring of benzene alone. "The high HOMO energy in the molecule confirms the donating ability of the glibenclamide molecule to unoccupied d-orbital of the metal indicating physical adsorption. The tendency of accepting electron from the surface of the metal was confirmed by the low LUMO energy. Moreover, the gap between LUMO and HOMO energies (ΔE) level of the molecule play a vital role in determining the efficiency of the inhibitor. The smaller the energy gap (ΔE), the more efficient is the inhibitor" [35, 36].

It has been reported by many researchers that, the reactivity of the chemical species depends on the energy gap, ΔE [25,40]. From the result in Table 4, the energy gap, ΔE of the glibenclamide molecule is -0.0927 eV. "The distribution of HOMO and LUMO is mainly situated at the nitrogen, and oxygen atoms in substituent groups. This kind of distribution

favors the parallel adsorption of amide derivative inhibitor onto the metal surface” [6,41]. This entails that the glibenclamide molecules donate and accept electrons from the Fe atom to form a back-donating bond [42, 54].

“The value of EHOMO was used in estimating the ionization energy, IE. In this case, Fe (in mild steel) and glibenclamide molecules are brought together, thus, electrons will flow from the lower system with lower electronegativity (inhibitor) to the system with higher electronegativity until the chemical potential becomes equal” [15,40, 43, 54]. The trend for the variation of inhibition potentials of the amide derivative agrees with experimental findings.

The measured polarity of a polar covalent bond is called the dipole moment, μ [44]. The negative total energy as shown in table 4 indicates that the glibenclamide molecules is a very stable molecule and is less prone to be broken apart. The dipole moment, μ of the glibenclamide molecules is 4716.06 Debye which is higher than that of H₂O (1.87 Debye) [28,44]. The adsorption between the glibenclamide molecules and metal surface is stronger probably due to the high values of dipole moment [49].

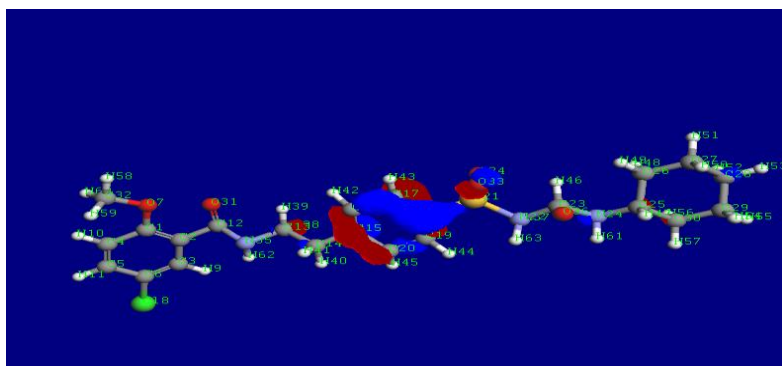


Figure 7: The Highest Occupied Molecular Orbital (HOMO) Density of Glibenclamide Molecule Using DFT at the RHF/STO-6G* Basis Set Level

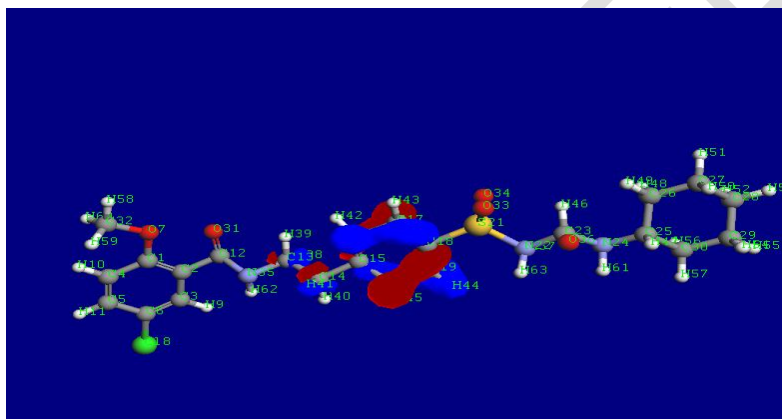


Figure 8: The Lowest Unoccupied Molecular Orbital (LUMO) Density of Glibenclamide Molecule Using DFT at the RHF/STO-6G* Basis Set Level

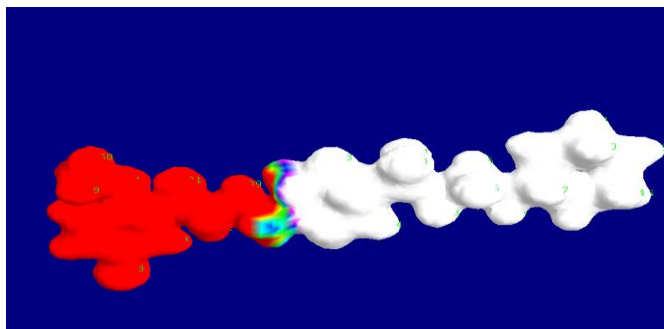


Figure 9: Molecular electrostatic potential-mapped density of Glibenclamide molecule

4.2.4 Mulliken population analysis

The more negative the atomic charges of the absorbed center are, the easier the atom donates electron to the unoccupied d-orbital of metal [45-47]. Table 5 shows the calculated Mulliken atomic charges for Glibenclamide molecule calculated using DFT at the RHF/STO-6G* basic level.

Table 5: Mulliken atomic charges for the Glibenclamide molecule (GLI)

Atom	Charge
1C	4.0000
2C	3.9999
3C	3.9968
4C	3.9999
5C	3.9978
6C	4.0210
7O	6.0000
8Cl	4.9830
9H	1.0009
10H	1.0000
11H	1.0006
12C	3.9980
13C	3.8303
14C	2.8051
15C	1.1614
16C	-0.1439
17C	-3.5616
18C	-3.9999
19C	-3.9987
20C	-2.5104
21S	-2.0001
22N	-3.0000
23C	-4.0000
24N	-3.0000
25C	-4.0000
26C	-4.0000
27C	-4.0000
28C	-4.0000
29C	-4.0000
30C	-4.0000
31O	5.9991
32C	4.0000
33O	-2.0000
34O	-2.0000
35N	4.9850

36O	-2.0000
37H	-1.0000
38H	0.9944
39H	0.9981
40H	0.9204
41H	0.9361
42H	0.4294
43H	-0.9988
44H	-1.0018
45H	0.1585
46H	-1.0000
47H	-1.0000
48H	-1.0000
49H	-1.0000
50H	-1.0000
51H	-1.0000
52H	-1.0000
53H	-1.0000
54H	-1.0000
55H	-1.0000
56H	-1.0000
57H	-1.0000
58H	1.0000
59H	1.0000
60H	1.0000
61H	-1.0000
62H	0.9997
63H	-1.0000

The result reveals that most of the Nitrogen atoms, all the Sulphur atoms, a few Hydrogen atoms, some Carbon and Oxygen atoms carry negative Mulliken charge densities, indicating possible sites of adsorption on the surface [49]. Moreover, some carbons atoms and most of the hydrogen atoms carry positive Mulliken charge densities. This specified the sites in which the molecules could accept electron from the metal un-occupied d-orbital as also reported by Eddy et al. [17].

4. CONCLUSION

The expired *Glucored Forte* drug was found to act as an effective corrosion inhibitor for mild steel in 2 M HCl solution and its inhibition efficiency related with different concentrations and chemical structures. Weight loss measurements were conducted at 303 K – 323 K to examine the corrosion inhibitive behavior of mild steel in 2 M HCl solution. The results confirmed that inhibitor efficiency had increased with increase in inhibitor concentration and decreased with increase in temperature and immersion time. The adsorption process of the expired *Glucored Forte* drug on mild steel surface favors a physical adsorption mechanism and is best described by the Temkin adsorption isotherm. The expired *Glucored Forte* drug adsorbed both as cationic species and molecular species as make known by quantum chemical analysis.

Disclaimer (Artificial intelligence)

Author(s) hereby declare that NO generative AI technologies such as Large Language Models (ChatGPT, COPILOT, etc) and text-to-image generators have been used during writing or editing of manuscripts.

REFERENCES

1. Sastri, V.S. Green corrosion inhibitors: theory and practice, John Wiley & Sons, 2012.
2. El-Etre, A.Y. Inhibition of C-steel corrosion in acidic solution using the aqueous extract of zallouh root, *Mater. Chem. Phys.* 2008;108 278–282.
3. Le Goff, G. Ouazzani, J. Natural hydrazine-containing compounds: Biosynthesis, isolation, biological activities and synthesis, *Bioorg. Med. Chem.* 2014;22 6529–6544.
4. Hosseini, M.G. Ehteshamzadeh, M.Shahrabi, T. Protection of mild steel corrosion with Schiff bases in 0.5 M H₂SO₄ solution, *Electrochim. Acta.* 2007; 52 3680–3685.
5. Thoume, A. Elmakssoudi, A. Left, D.B.Benzbiria, N. Benhiba, F. Dakir, M.Zahouily, M. Zarrouk, A. Azzi, M.Zertoubi, M.Amino acid structure analog as a corrosion inhibitor of carbon steel in 0.5 M H₂SO₄: Electrochemical, synergistic effect and theoretical studies, *Chem. Data Collect.* 2020;30 100586.
6. Solomon, M.M. Essien, K.E. Loto, R.T.. Ademosun, O.T Synergistic corrosion inhibition of low carbon steel in HCl and H₂SO₄ media by 5-methyl-3-phenylisoxazole-4-carboxylic acid and iodide ions, *J. Adhes. Sci. Technol.* 2022;36 1200–1226.
7. Glaser, R. Lewis, M. Wu, Z. Stereochemistry and stereoelectronics of azines. 13. Conformational effects on the quadrupolarity of azines. An ab initio quantum-mechanical study of a lateral synthon, *Mol. Model. Annu.* 2000;6 86–98.
8. Yadav, M. Gope, L. Kumari, N. Yadav, P. Corrosion inhibition performance of pyranopyrazole derivatives for mild steel in HCl solution: Gravimetric, electrochemical and DFT studies, *J. Mol. Liq.* 2016; 216 78–86.
9. El Arrouji, S. Alaoui, K.I. Zerrouki, A. Kadiri, S.E.L. Touzani, R. Rais, Z. Baba, M.F. Taleb, M. Chetouani, A. Aouniti, A. The influence of some pyrazole derivatives on the corrosion behaviour of mild steel in 1M HCl solution, *J. Mater. Environ. Sci.* 2016;7 299–309.
10. El Arrouji, S. Karrouchi, K. Berisha, A. Alaoui, K.I. Warad, I. Rais, Z. Radi, S. Taleb, M. Zarrouk, A. New pyrazole derivatives as effective corrosion inhibitors on steel-electrolyte interface in 1 M HCl: Electrochemical, surface morphological (SEM) and computational analysis, *Colloids Surfaces A Physicochem. Eng. Asp.* 2020;604 125325.
11. Umoren, S.A. Inhibition of aluminium and mild steel corrosion in acidic medium using Gum Arabic, *Cellulose.* 2008;15 751–761. <https://doi.org/10.1007/s10570-008-9226-4>.
12. Umoren, S.A. Synergistic inhibition effect of polyethylene glycol–polyvinyl pyrrolidone blends for mild steel corrosion in sulphuric acid medium, *J. Appl. Polym. Sci.* 2011;119, 2072–2084. <https://doi.org/10.1002/app.32922>.
13. Chauhan, D.S. Quraishi, M.A. Qurashi, A. Recent trends in environmentally sustainable Sweet corrosion inhibitors, *J. Mol. Liq.* 2021; 326, 115117.
14. Oguzie, E.E. Adindu, C.B. Enenebeaku, C.K. Ogukwe, C.E. Chidiebere, M.A. Oguzie, K.L. Natural products for materials protection: mechanism of corrosion inhibition of mild steel by acid extracts of Piper guineense, *J. Phys. Chem. C.* 2012;116, 13603–13615. <https://doi.org/10.1021/jp300791s>.
15. Ebenso, E.E. Isabirye, D.A. Eddy, N.O. Adsorption and quantum chemical studies on the inhibition potentials of some thiosemicarbazides for the corrosion of mild steel in acidic medium, *Int. J. Mol. Sci.* 2010;11, 2473–2498. <https://doi.org/10.3390/ijms11062473>.
16. Eddy, N.O. Momoh-Yahaya, H. Oguzie, E.E. Theoretical and experimental studies on the corrosion inhibition potentials of some purines for aluminum in 0.1 M HCl, *J. Adv. Res.* 2015; 6, 203–217. <https://doi.org/10.1016/j.jare.2014.01.004>.

17. Eddy, N.O. Ebenso, E.E. Ibok, U.J. Adsorption, synergistic inhibitive effect and quantum chemical studies of ampicillin (AMP) and halides for the corrosion of mild steel in H₂SO₄, *J. Appl. Electrochem.* 2010; 40, 445–456. <https://doi.org/10.1007/s10800-009-0015-z>.
18. Kousar, K. Walczak, M.S. Ljungdahl, T. Wetzel, A. Oskarsson, H. Restuccia, P. Ahmad, E.A. Harrison, N.M. Lindsay, R. Corrosion inhibition of carbon steel in hydrochloric acid: Elucidating the performance of an imidazoline-based surfactant, *Corros. Sci.* 2021;180, 109195.
19. Khaled, K.F. Abdel-Rehim, S.S. Sakr, G.B. On the corrosion inhibition of iron in hydrochloric acid solutions, Part I: Electrochemical DC and AC studies, *Arab. J. Chem.* 2012;5, 213–218. <https://doi.org/10.1016/j.arabjc.2010.08.015>.
20. Obi-Egbedi, N.O. Essien, K.E. Obot, I.B. Computational simulation and corrosion inhibitive potential of alloxazine for mild steel in 1M HCl, *J. Comput. Methods Mol. Des.* 2011; 1, 26–43.
21. Obot, I.B. Obi-Egbedi, N.O. Odozi, N.W. Acenaphtho [1, 2-b] quinoxaline as a novel corrosion inhibitor for mild steel in 0.5 M H₂SO₄, *Corros. Sci.* 2010; 52, 923–926. <https://doi.org/10.1016/j.corsci.2009.11.013>.
22. Tang, L. Li, X. Mu, G. Liu, G. Li, L. Liu, H. Si, Y. The synergistic inhibition between hexadecyl trimethyl ammonium bromide (HTAB) and NaBr for the corrosion of cold rolled steel in 0.5 M sulfuric acid, *J. Mater. Sci.* 2006; 41, 3063–3069. <https://doi.org/10.1007/s10853-006-6987-8>.
23. Obot, I.B. Obi-Egbedi, N.O. Fluconazole as an inhibitor for aluminium corrosion in 0.1 M HCl, *Colloids Surfaces a Physicochem. Eng. Asp.* 2008;330, 207–212. <https://doi.org/10.1016/j.colsurfa.2008.07.058>.
24. Njoku, D.I. Onuoha, G.N. Oguzie, E.E. Oguzie, K.L. Egbedina, A.A. Alshwabkeh, A.N. Nicotiana tabacum leaf extract protects aluminium alloy AA3003 from acid attack, *Arab. J. Chem.* 2019; 12, 4466–4478. <https://doi.org/10.1016/j.arabjc.2016.07.017>.
25. Jackson, E. Essien, K.E. Experimental and Theoretical Approach of L-Methionine Sulfone (LMS) as corrosion inhibitor for mild steel in HCL Solution, *Environment.* 2019;1, 2.
26. Paul, P.K. Yadav, M. Obot, I.B. Investigation on corrosion protection behavior and adsorption of carbohydrazide-pyrazole compounds on mild steel in 15% HCl solution: Electrochemical and computational approach, *J. Mol. Liq.* 2020;314, 113513.
27. Hosseini, S.M.A.Salari, M. Jamalizadeh, E. Khezripor, S. Seifi, M. Inhibition of mild steel corrosion in sulfuric acid by some newly synthesized organic compounds, *Mater. Chem. Phys.* 2010; 119, 100–105. <https://doi.org/10.1016/j.matchemphys.2009.08.029>.
28. Essien, K.E. Odiongeyi, A. O. Ekerete, J. B. Okon, E. O. Idongesit, E. O. Nnabuk O. E. Abai, E.J. Corrosion Inhibition Potential of Two Isoxazole Derivatives: Experimental and Theoretical Analyses, *Mater. Environ. Sci.*, 2022, 13 (8), 928-944.
29. Dohare, P. Quraishi, M.A. Verma, C. Lgaz, H. Salghi, R. Ebenso, E.E. Ultrasound induced green synthesis of pyrazolo-pyridines as novel corrosion inhibitors useful for industrial pickling process: Experimental and theoretical approach, *Results Phys.* 2019; 13, 102344.
30. Fouda, A.S. Abd El-Aal, A. Kandil, A.B. The effect of some phthalimide derivatives on corrosion behavior of copper in nitric acid, *Desalination.* 2006;201 216–223. <https://doi.org/10.1016/j.desal.2005.11.030>.
31. Jackson, E. Essien, K.E. Okafor, P.C. Experimental and Quantum Studies: A New Corrosion Inhibitor for Mild Steel, *Elixir Corrosion and Dye*, 2016; 90, 37673-3767
32. Verma, C. Saji, V.S. Quraishi, M.A. Ebenso, E.E. Pyrazole derivatives as environmental benign acid corrosion inhibitors for mild steel: experimental and computational studies, *J. Mol. Liq.* 2020;298, 111943.
33. Ouchrif, A. Zegmout, M. Hammouti, B. El-Kadiri, S. Ramdani, A.1, 3-Bis (3-hydroxymethyl-5-methyl-1-pyrazole) propane as corrosion inhibitor for steel in 0.5 M H₂SO₄ solution, *Appl. Surf. Sci.* 2005;252 339–344.

34. El Ouadi, Y.Lamsayah, M.Bendaif, H.Benhiba, F. Touzani, R.Warad, I.Zarrouk, A.Electrochemical and theoretical considerations for interfacial adsorption of novel long chain acid pyrazole for mild steel conservation in 1 M HCl medium, *Chem. Data Collect.* 2021;31, 100638.
35. Obi-Egbedi, N.O. Essien, K.E. Obot, I.B. Ebenso, E.E. 1, 2-Diaminoanthraquinone as corrosion inhibitor for mild steel in hydrochloric acid: weight loss and quantum chemical study, *Int. J. Electrochem. Sci.* 2011;6, 913–930.
36. Abd El Rehim, S.S. Ibrahim, M.A.M. Khalid, K.F. The inhibition of 4-(2'-amino-5'-methylphenylazo) antipyrine on corrosion of mild steel in HCl solution, *Mater. Chem. Phys.* 2001; 70, 268–273. [https://doi.org/10.1016/S0254-0584\(00\)00462-4](https://doi.org/10.1016/S0254-0584(00)00462-4).
37. Soltani, N. Tavakkoli, N. Kashani, M.K. Mosavizadeh, A. Oguzie, E.E. Jalali, M.R. Silybum marianum extract as a natural source inhibitor for 304 stainless steel corrosion in 1.0 M HCl, *J. Ind. Eng. Chem.* 2014;20 3217–3227. <https://doi.org/10.1016/j.jiec.2013.12.002>.
38. Emranuzzaman, T. Kumar, S. Vishwanatham, G. U. Synergistic effects of formaldehyde and alcoholic extract of plant leaves for protection of N80 steel in 15% HCl, *Corros. Eng. Sci. Technol.* 2004;39, 327–332. <https://doi.org/10.1179/174327804X13181>.
39. Li, X. Deng, S. Xie, X. Fu, H. Inhibition effect of bamboo leaves' extract on steel and zinc in citric acid solution, *Corros. Sci.* 2014; 87,15–26. <https://doi.org/10.1016/j.corsci.2014.05.013>.
40. Eddy, N.O. Experimental and theoretical studies on some amino acids and their potential activity as inhibitors for the corrosion of mild steel, part 2, *J. Adv. Res.* 2011;2 35–47. <https://doi.org/10.1016/j.jare.2010.08.005>.
41. Yadav, M. Behera, D. Kumar, S.Experimental and theoretical studies on corrosion inhibition of mild steel in hydrochloric acid by thiosemicarbazone of Schiff bases, *Can. Metall. Q.* 2014; 53, 220–231. <https://doi.org/10.1179/1879139513Y.0000000118>.
42. Deng, S. Li, X. Xie, X. Hydroxymethyl urea and 1, 3-bis (hydroxymethyl) urea as corrosion inhibitors for steel in HCl solution, *Corros. Sci.* 2014; 80, 276–289. <https://doi.org/10.1016/j.corsci.2013.11.041>.
43. Obot, A.S. BoEKOM, E.J. ITUEN, E.B. UGI, B.U. ESSIEN, K.E. JONAH, N.B. THERMODYNAMIC INVESTIGATION AND QUANTUM CHEMICAL EVALUATION OF n-HEXANE EXTRACTS OF *Costuslucanusianus* AS CORROSION INHIBITORS FOR MILD STEEL AND ALUMINUM IN 1 M HCl SOLUTION, *J. Appl. Phys. Sci. Int.* 2021;13, 6–27.
44. Eddy, N.O.Part 3. Theoretical study on some amino acids and their potential activity as corrosion inhibitors for mild steel in HCl, *Mol. Simul.* 2010;36, 354–363. <https://doi.org/10.1080/08927020903483270>.
45. Misawa, T. Asami, K. Hashimoto, K.Shimodaira, S.The mechanism of atmospheric rusting and the protective amorphous rust on low alloy steel, *Corros. Sci.* 1974;14, 279–289.
46. Misawa, T. Kyuno, T.Suetaka, W.Shimodaira, S.The mechanism of atmospheric rusting and the effect of Cu and P on the rust formation of low alloy steels, *Corros. Sci.* 1971; 11, 35–48.
47. Ganesan, A.R. Subramani, K. Shanmugam, M.Seedevi, P. Park, S.Alfarhan, A.H. Rajagopal, R. Balasubramanian, B.A comparison of nutritional value of underexploited edible seaweeds with recommended dietary allowances, *J. King Saud Univ.* 2020; 32, 1206–1211.
48. Ishii, M. Nakahira, M. Yamanaka, T.Infrared absorption spectra and cation distributions in (Mn, Fe)₃O₄, *Solid State Commun.* 1972; 11, 209–212.
49. Ikot, A. N. Akpabio, L. E. Essien, K. Ituen E. E. Obot. I. B. Variational Principle Techniques and the Properties of a Cut-off and Anharmonic Wave Function, *E-Journal of Chemistry*, 2009; 6(1), 113-119.
50. Udeh B. C., Nwanyibuife NA, Monday O. Inhibition of Aluminium Corrosion in KOH Solution Using Extract of Grape Leaf as Inhibitor. *J. Mater. Sci. Res. Rev. [Internet]*. 2023 Nov. 11 [cited 2024 Jun. 15];6(4):803-11. Available from: <https://journaljmsrr.com/index.php/JMSRR/article/view/289>

51. Khalil SM, Al-Mazaideh GM, Ali NM. DFT calculations on corrosion inhibition of Aluminum by some carbohydrates. *Int J Biochem Res Rev.* 2016; 14(2):1-7.
52. Raja, P. B. Sethuraman MG. Natural products as corrosion inhibitor for metals in corrosive media—a review. *Materials letters.* 2008; 62(1):113-6
53. Gece G. The use of quantum chemical methods in corrosion inhibitor studies. *Corrosion science.* 2008; 50(11): 2981-92.
54. Essien, K. E., Okon, E. J., Archibong, I.N., Okon, O. E., George, I. E. Experimental, Quantum Chemical And IR Spectroscopy Studies on the Corrosion Inhibition of Mild Steel by 3,5-Dimethyl-4-Nitroisoxazole in HCl Solutions. *J. Mater. Environ. Sci.*, 2024; 15 (1), 136-150
56. Ahamad, I., Prasad, R., Quraishi, M. A. Experimental and theoretical investigations of adsorption of fexofenadine at mild steel/hydrochloric acid interface as corrosion inhibitor. *Journal of Solid State Electrochemistry*, 2010; 14, 2095-2105.
57. Mehdaoui R, Khelifa A, Khadraoui A, Aaboubi O, Hadj Ziane A, Bentiss F, Zarrouk A. Corrosion inhibition of carbon steel in hydrochloric acid solution by some synthesized surfactants from petroleum fractions. *Research on Chemical Intermediates.* 2016; 42:5509-26.
58. Obi-Egbedi NO, Obot IB. Adsorption behavior and corrosion inhibitive potential of xanthene on mild steel/sulphuric acid interface. *Arabian Journal of Chemistry.* 2012; 5(1):121-33.
59. Martin A, Silva V, Perez L, García-Serna J, Cocero MJ. Direct synthesis of linalyl acetate from linalool in supercritical carbon dioxide: a thermodynamic study. *Chemical Engineering & Technology: Industrial Chemistry-Plant Equipment-Process Engineering-Biotechnology.* 2007; 30(6):726-31.
60. El-Haddad MN, Fouda AS, Hassan AF. Data from chemical, electrochemical and quantum chemical studies for interaction between Cephapirin drug as an eco-friendly corrosion inhibitor and carbon steel surface in acidic medium. *Chemical Data Collections.* 2019; 22:100251.
61. Hameed RS, Aljohani MM, Essa AB, Khaled A, Nassar AM, Badr MM, Al-Mhyawi SR, Soliman MS. Electrochemical techniques for evaluation of expired megavit drugs as corrosion inhibitor for steel in hydrochloric acid. *International Journal of Electrochemical Science.* 2021;16(4):210446.
62. Obot IB, Obi-Egbedi NO, Eseola AO. Anticorrosion potential of 2-mesityl-1H-imidazo [4, 5-f][1, 10] phenanthroline on mild steel in sulfuric acid solution: experimental and theoretical study. *Industrial & engineering chemistry research.* 2011;50(4):2098-110.